The influence of environmental setting on the community ecology of Ediacaran organisms

Emily G. Mitchell[1], *Nikolai Bobkov*[2,3], *Natalia Bykova*[2,4], *Alavya Dhungana*,[5], *Anton Kolesnikov*[2,6,7], *Ian R. P. Hogarth*[8,9] *Alexander G. Liu*[10], *Tom M.R. Mustill*[10,11], *Nikita Sozonov*[2,3], *Vladimir Rogov*[2], *Shuhai Xiao*[4] *and Dmitriy V. Grazhdankin*[2,3]

ek338@cam.ac.uk

[1]Department of Zoology, University of Cambridge, UK.

[2]Trofimuk Institute of Petroleum Geology and Geophysics, Novosibirsk, Russian Federation.

[3]Novosibirsk State University, Russian Federation.

[4]Department of Geosciences, Virginia Tech, Blacksburg, VA 24061, United States.

[5] Department of Earth Sciences, Durham University, UK.

[6]Geological Institute, Russian Academy of Sciences, Moscow, Russian Federation.

[7]Department of Geography, Moscow Pedagogical State University, Moscow, Russian Federation.

[8]Department of Chemical Engineering, University of Cambridge, UK.

[9]Current address: University College London, UCL Institute for Innovation and Public Purpose, UK.

[10]Department of Earth Sciences, University of Cambridge, UK.

[11]Current address: Gripping Films, St. John's Church Road, London, England, E9 6EJ.

Abstract

The broad-scale environment plays a substantial role in shaping modern marine ecosystems, but the degree to which palaeocommunities were influenced by their environment is unclear. To investigate how broad-scale environment influenced the community ecology of early animal ecosystems, we employed spatial point process analyses (SPPA) to examine the community structure of seven bedding-plane assemblages of late Ediacaran age (558–550 Ma), drawn from a range of environmental settings and global localities. The studied palaeocommunities exhibit marked differences in the response of their component taxa to sub-metre-scale habitat heterogeneities on the seafloor. Shallow-marine (considered here as above storm wave-base) palaeocommunities were heavily influenced by local habitat heterogeneities, in contrast to their deeper-water counterparts. The local patchiness within shallow-water communities may have been further accentuated by the presence of grazers and detritivores, whose behaviours potentially initiated a chain of increasing habitat heterogeneity of benthic communities from shallow to deep-marine depositional environments. Higher species richness in shallow-water Ediacaran assemblages compared to deep-water counterparts across the studied time-interval could have been driven by this environmental patchiness, because habitat heterogeneities increase species richness in modern marine environments. Our results provide quantitative support for the "Savannah" hypothesis for early animal diversification – whereby Ediacaran diversification was driven by patchiness in the local benthic environment.

Keywords

Ediacaran, palaeoecology, spatial analysis, early animal diversification.

Author Contributions

E. Mitchell conceived this paper and wrote the first draft. N. Bobkov, A. Kolesnikov, N. Sozonov and D. Grazhdankin collected the data for DS surface. N. Bobkov and N. Sozonov

performed the analyses on DS surface. N. Bykova, S. Xiao, and D. Grazhdankin collected the data for KH1 and KH2 surfaces, and N. Bykova and D. Grazhdankin collected the data for WS-A, and E. Mitchell performed the analyses. A. Dhungana and A. Liu collected the data for FUN4 and FUN5 surfaces and A. Dhungana performed the analyses. T. Mustill and D. Grazhdankin collected the data for KS and T. Mustill and E. Mitchell performed the analyses. I. Hogarth developed the software for preliminary KS surface analyses. V. Rogov conducted the sedimentological study of the Khatyspyt Formation. E. Mitchell, N. Bobkov, N. Bykova, A. Dhungana, A. Kolesnikov, A. Liu, S. Xiao and D. Grazhdankin discussed the results and prepared the manuscript.

Background

The Ediacaran–Cambrian transition (~580–520 million years ago) is one of the most remarkable intervals in the history of life on Earth, witnessing the rise of macroscopic, complex animals in the global oceans (1,2). The diversification of early animals coincides with dramatic perturbations in the global environment, including changes to carbon cycling and a progressive but dynamic oxygenation of the oceans (3,4). The extent to which animals themselves drove these global changes is a matter of considerable debate (5–7). Competing hypotheses suggested to explain the observed environmental shifts include global abiotic changes that occured over kilometre scales (8,9) and biotic factors acting over local scales (metre to kilometre), and include organism interactions such as burrowing and/or predation (10,11). Feedbacks between biotic and abiotic factors have also been proposed as drivers of early animal diversification, whereby Ediacaran organisms directly or indirectly created patchy food resources, stimulating the evolution of mobile bilaterians (12,13). Due to the small (within community) spatial scales over which key evolutionary mechanisms often act (14), investigation of the community ecology of Ediacaran assemblages from sites large distances (kilometres) apart offers an

opportunity to link the interactions of individual organisms to macro-evolutionary and macro-ecological trends. In this study, we investigate the relationship between late Ediacaran early animal diversification and the broad-scale environment.

Ediacaran macrofossils occur globally across a wide-range of palaeo-environments (1). Previous studies have separated late Ediacaran palaeocommunities into three taxonomically distinct assemblages – the Avalon, White Sea and Nama – which occupy partially overlapping temporal intervals and water-depths, with no significant litho-taphonomic or biogeographic influence (15–17). This study focusses on palaeocommunities within the Avalon and White Sea fossil assemblages. Since these are considered to reflect original *in situ* communities (18,19), they permit the use of statistical analysis of the distribution of fossil specimens on bedding planes (spatial point process analyses, SPPA) to reconstruct the interaction of organisms with each other and their local environment (20–25). The Avalon assemblage is primarily represented by sites in Newfoundland (Canada) and Charnwood Forest (UK) (26,27), and typically documents mid-shelf/deep-water settings (from depths below the storm-wave base) of ~571–557 Ma (28,29). Such sites exhibit relatively limited ecological and morphological diversity (30,31), and palaeocommunities consist almost exclusively of sessile taxa (32) that show only weak trends in community composition along regional palaeoenvironment gradients (20). Previous spatial analyses of Avalonian palaeocommunities have found limited evidence for environmental interactions within these communities (21,23), in contrast to the strong imprint exerted by resource-limitation on modern deep-sea ecosystems (33,34).

Palaeocommunities from the White Sea assemblage are most famously represented by sites in South Australia, and the East European Platform of Russia, dating to ~558–550 Ma (35–37).

These assemblages typically document shallow-water, diverse communities including some of the oldest candidate bilaterians, with taxa interpreted to exhibit a wide range of ecological strategies (7,12,36,38). Within the White Sea assemblages, community composition is strongly correlated with facies and the presence of textured organic surfaces at bed-scale level (39,40).

Metrics of taxonomic and ecological diversity are much higher in White Sea assemblages than in Avalonian ones, with changes in taxonomic and morphological diversity calculated to be of similar magnitude to those between the Ediacaran and Cambrian (30,31). These Ediacaran assemblages have high beta-diversity compared to modern benthic systems (41), but the driving processes underlying this high diversity are not understood. The regional palaeoenvironment (kilometre scale) (15,17) has a significant influence on (non-algal dominated) Ediacaran fossil assemblage composition, but its influence on local (metre to sub-metre scale) community ecology has not yet been investigated. In modern benthic communities, small spatial scale (< 50 cm) substrate heterogeneities (e.g. substrate variations in nutrients, oxygen patchiness, or biotic and abiotic gradients within microbial mats) exert a significant influence on community ecology (33,34,42). For Ediacaran palaeocommunities, it is not possible from spatial analyses alone to determine the underlying causes of habitat heterogeneities, nor the extent to which they relate to food resources, such as those resulting from the decay of Ediacaran organisms (12,43). However, it is possible to compare how the relative influence of such heterogeneities changes with broad-scale environmental setting: previous analyses have identified assemblage-level trends between community compositions and bathymetric depth (15–17). In this study, we compare the drivers of community ecology between shallow and deep-water Ediacaran palaeocommunities (above or below the storm-wave-base) over a ~8 million-year period using spatial analyses of seven palaeocommunities.

Spatial analyses

Determining the nature of interactions between fossilised organisms and their environment can be undertaken if entire palaeocommunities are preserved *in situ*, such that the position of a fossil on a bedding plane can be interpreted to reflect aspects of the original organism's life-history (44). For sessile organisms, such as in the Avalon communities, community-scale spatial distributions are dependent upon the interplay of a limited number of factors: physical environment (which manifests as habitat associations of a taxon or taxon-pairs (45)); organism dispersal/reproduction (46); competition for resources (47); facilitation between taxa (where one taxon increases the survival another taxon) (48); and differential mortality (49). For fossil assemblages containing mobile taxa (e.g. the White Sea assemblages), behavioural ecology also influences spatial distributions, so interpretations of their spatial distributions are necessarily qualitative rather than quantitative.

Studies of modern ecosystems have demonstrated that habitat associations resulting from interactions between organisms and their local environment can be either positive, leading to aggregations of individuals (such as around a preferential substrate for establishment), or negative segregation away from such patches (21). SPPA are a suite of analyses which compare the relative density of points (in this case fossil specimens) to different models corresponding to different ecological processes, in order to infer the most likely underlying process responsible for producing the observed spatial distribution (44,50). The application of SPPA to Ediacaran palaeocommunities is documented in detail in the Methods section (see also 21–23,25,50). For sessile organisms, habitat associations identified by SPPA are best-modelled by a heterogeneous Poisson model (HP), or when combined with dispersal limitations, an Inhomogeneous Thomas Cluster model (ITC) . Where the local environment is

resource-limited to the extent that it significantly reduces organism densities, this is indicated by spatial segregation between specimens within a community . When sessile populations are not significantly affected by their local environment, their spatial distributions are completely spatially random (CSR), indicating no significant influence by any biological or ecological processes at the spatial scale investigated (45,52–55). Alternatively, sessile populations which are not CSR and not affected by their local environment reflect dispersal/reproductive processes (45,52–55). CSR is modelled by homogeneous Poisson processes (44), whereas dispersal patterns are best modelled by best-fit Thomas Cluster (TC) or Double Thomas Cluster (DTC) models (52). Facilitation (where one taxon increases the survival of another) is best-modelled by linked-cluster models and density-dependent processes are detected using random-labeling analyses .

Geological setting

We assessed the community palaeoecology of seven fossil-bearing assemblages across five different global Ediacaran locations (Table 1, Figs 1, S1), spanning a range of habitats (Fig. S2) inhabited by members of the Ediacaran soft-bodied macrobiota during the late Ediacaran interval. Data from these assemblages were compared with seven palaeocommunities that have been subjected to SPPA in previous studies (see (21,23) for details of data collection and locality information). The diverse local depositional environments represented by these combined localities are here coarsely grouped within either shallow or deep-water settings, with deep-water defined as those surfaces below storm-wave base, to permit us to focus attention on the broadest macro-ecological and macro-evolutionary patterns in the data.

Shallow marine settings

Five of the studied palaeocommunities are found in facies that reflect a relatively shallow marine wave and current-agitated depositional environments. Palaeocommunity WS-A (White Sea) is an *Aspidella*–bearing surface (Fig. 1E) on the underside of a 15–30-mm-thick wave-rippled sandstone which forms part of a thick package of alternating wave-bedded sandstones, siltstones and mudstones interpreted as a product of progressive sediment-sorting by waves within a prograding, storm-influenced shoreface depositional system (Fig. S2; 55,56). It was collected from the Lyamtsa Formation of the Valdai Group, along the Onega Coast of the White Sea, Russian Federation. The original complete surface was studied in the field, where it has since been destroyed by landslides. *Aspidella* specimens were collected and are stored uncatalogued at the Trofimuk Institute for Petroleum Geology and Geophysics in Novosibirsk. The Lyamtsa Formation is older than a date of 558 ± 1 Ma (U/Pb zircon dating of volcanic tuffs near the base of the overlying Verkhovka Formation) (16).

Surface (KS) (Fig. 1A) originates from a section comprising 1.3–3.2 m thick, laterally continuous fining-upward sequences. Each sequence begins with channel casts or thick (0.5–0.6 m) packages of laterally discontinuous fossiliferous thin-bedded sandstones often exhibiting soft-sediment deformations (Fig. S2). These are followed by a package (0.4–0.7 m) of interbedded thinner wave-rippled sandstones, progressively thinning towards the top of the package. The upper part of each sequence is represented by an interval of alternating siltstone and shale. This section is interpreted as a prograding flood-influenced prodelta depositional system, and is part of the lower member of the Erga Formation (Winter Coast of the White Sea) (16,35), which is younger than 552.85 ± 0.77 Ma (58) (date recalculated from Martin et al. (59)). The KS surface was documented in the field and has been subsequently destroyed by landslides and weathering.

Two *Funisia*-bearing surfaces (Fig. 1D) from oscillation-rippled quartz-sandstones (the 'ORS' facies of (60)) are interpreted to have been deposited between fair-weather and storm-wave base under oscillatory and combined flow in the Ediacara Member of South Australia (39,61–63). These surfaces reside in the collections of the South Australia Museum, with surface FUN4 collected from Ediacara Conservation Park (SAM P55236) and surface FUN5 collected from the Mount Scott Range (SAM P41506). Since FUN4 and FUN5 originate from different localities (> 50 km apart), it is assumed likely that they represent discrete bedding plane palaeocommunities. The South Australian Ediacaran successions have not been radiometrically dated, but the Ediacara Member is widely assumed to be of a similar age to the Russian White Sea fossil-bearing sections (1,2).

Surface DS is a *Dickinsonia*-bearing surface (Fig. 1B) from the Konovalovka Member of the Cherny Kamen Formation, cropping out along the Sylvitsa River, Central Urals, Russian Federation (64,65). It lies within an interval of finely alternating wave-rippled sandstones, siltstones and mudstones that are sandwiched between two thick intervals of biolaminated sandstone characterised by microbial shrinkage cracks and salt crystal pseudomorphs (66). The overall succession is considered transitional from marginal marine to non-marine, with the fossil-bearing interval interpreted as having been deposited in a lagoon within a tidal flat depositional system (66). A U/Pb zircon date of 557 ± 13 Ma from volcanic tuffs near the base of the Cherny Kamen Formation (65) suggests that this unit may have been deposited broadly coevally with those on the White Sea coast. Specimens from this surface reside in Novosibirsk State University, Russian Federation (specimen numbers: 2057-001 to 2057-003) and will be placed at the Ural Geological Museum (Yekaterinburg).

All five of these surfaces, therefore, represent siliciclastic depositional environments from above the storm-wave base (Fig S2), and so fall broadly into the grouping of "shallow

marine". They contain examples of taxa interpreted as animals (e.g. *Dickinsonia* (67), *Kimberella* (68)) as well as non-metazoans (*Orbisiana*) (69), and their age and facies place them within the White Sea assemblage (15,17).

Deep marine settings

Two bedding surfaces dominated by *Aspidella* specimens (KH1 and KH2, Fig. 1C) were collected from a package of finely alternating limestone and shale interbeds within the uppermost Khatyspyt Formation, Khorbusuonka River, Siberia. The Khatyspyt Formation records a relatively narrow basin with steep slopes developed in a marine ramp setting (Fig. S2). Sedimentological observations (e.g., turbiditic nature of the limestones; evidence of strong unidirectional flows; intraclasts originating from outside of the Khatyspyt depositional basin) suggest the Khatyspyt Formation was deposited within a starved intracratonic rift, beyond the flexure slope break (70–73). The lack of any evidence of wave reworking within the entire Khatyspyt Formation, and the geochemical evidence of stratification and anoxia (74), with episodic euxunia, corroborate a deep-water interpretation of the Khatyspyt depositional environment. A positive $\delta^{13}C_{carb}$ excursion in the Khatyspyt Formation has been correlated with an excursion of similar magnitude in the <550 Ma Gaojiashan Member of the Dengying Formation (73). Strontium isotope ratios ($^{87}Sr/^{86}Sr$) in the Khatyspyt Formation are consistently ca. 0.7080 (73,74), a value approaching some of the ratios seen in the Gaojiashan Member (75), so this correlation seems plausible. Surface KH2 remains in the field, and surface KH1 was destroyed by excavating surface KH2. Specimens from surface KH1 reside in Trofimuk Institute for Petroleum Geology and Geophysics, collection number 913 (specimen numbers: 0607/2009-3, 0607/2009-6, 0607/2009-7, 0607/2009-17, 0607/2009-18).

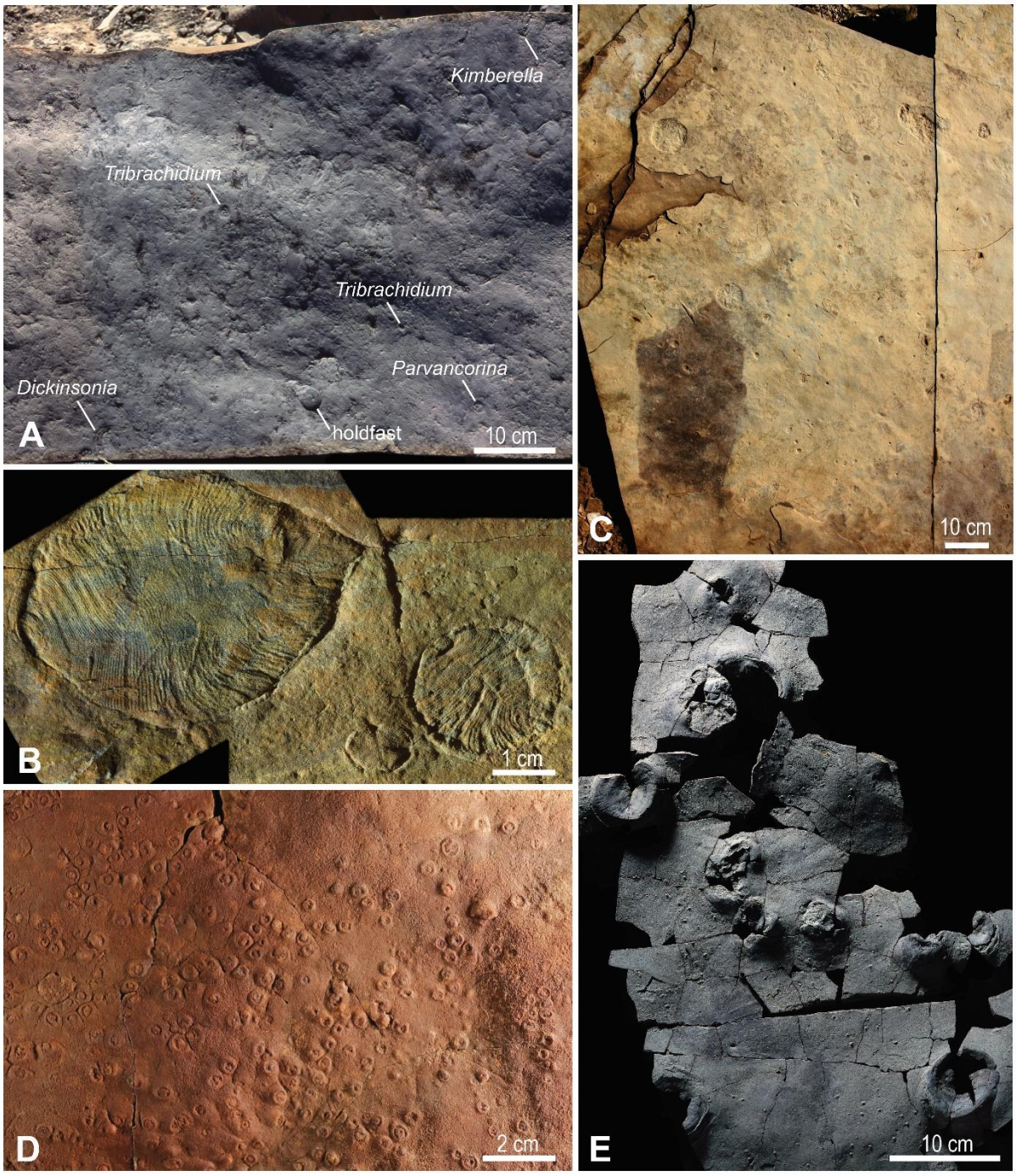

Fig. 1. Assemblages of Ediacaran fossils from study localities. A) A fragment of the *Kimberella* surface (KS), indicating key taxa, lower Erga Formation, Winter Coast of the White Sea. B) Specimens of *Dickinsonia* from the *Dickinsonia* surface (DS), Konovalovka Member, Cherny Kamen Formation, Sylvitsa River, Central Urals. C) A representative fragment of the *Aspidella* surface (KH1), Khatyspyt Formation, Olenek Uplift, Northern Siberia. D) *Funisia* from FUN4 surface (SAM P55236), Ediacara Member, Rawnsley Quartzite, South Ediacara

Conservation Park, Flinders Ranges, South Australia. E) A representative fragment of the WS-A surface, upper Lyamtsa Formation, White Sea Region. This particular fragment was not included in the analysis.

Data Collection

Spatial data were collected from the surfaces using different methods depending on the physical properties of the bedding plane (Table 1). The WS-A, KH1, KH2 surfaces were mapped in the field (WS-A in 2017, KH1 in 2006 and 2009, and KH2 in 2018) onto millimetre graph paper (Fig. 2). First, the co-ordinates of the edge of the rock surface were recorded, then the co-ordinates, orientation and dimensions of each of the specimen were measured and plotted onto the paper. For DS, a bedding surface of 9 m^2 was excavated over the course of two years (2017–2018). The surface was photo-mapped, with photographs taken under an artificial light source at night. The intersection between maximum length (L) and maximum width (W) of each specimen was taken to be the absolute position of the organism, with measurements obtained from digital photographs using Adobe Photoshop CC software and Apple Script Editor (Fig. 2).

Surface	Environmental setting	Species richness	Dominant Taxon/taxa	Specimen numbers	Area mapped (m^2)
WS-A	Shallow	1	*Aspidella*	40	0.54
KH1	Deep	2	*Aspidella*	204	2.38
KH2	Deep	2	*Aspidella*	81	1.52
DS	Shallow	1	*Dickinsonia*	62	9.00
KS	Shallow	13	*Kimberella*, *Orbisiana*	107	2.74
FUN4	Shallow	2	*Funisia*	290	0.69
FUN5	Shallow	1	*Funisia*	482	0.78

Table 1. Summary data of the surfaces mapped. The environmental setting, species richness, specimen numbers within the mapped area, and the total mapped area are provided.

The KS surface was excavated in July 2004, and is a laterally discontinuous transect consisting of four slabs of variable size, ranging from 0.6 × 0.4 m to 1.6 × 1.0 m. The relative positions of the slabs within the transect were mapped *in situ* on an excavated terrace. A separate block originating from the same horizon was found in float close to the transect. Following reassembly, the taxonomic identity, positions, orientations and shapes of the fossils were mapped at millimetre scale (Fig. 2). For the FUN4 and FUN5 surfaces, photogrammetric maps of the bedding surfaces were made, with lens edge effects corrected using RawTherapee (v. 2.4.1; Fig. 2). For all mapped palaeocommunities, fossil identification, position, and dimensions (disc width, disc length, stem length, stem width, frond length, and frond width) were digitized in Inkscape 0.92.3 on a 2D projection of the dataset, resulting in a 2D vector map for each palaeocommunity (Fig. 2). Only taxa that had sufficient abundance (> 5 specimens) for spatial analyses were formally identified, and these were grouped within one of six taxonomic groups: *Aspidella*, *Dickinsonia*, *Funisia*, *Kimberella*, *Orbisiana,* and the trace fossil *Kimberichnus*. *Aspidella* is considered a form taxon here, in line with previous studies (66,80), and may represent multiple different types of organism, such as the holdfasts of frondose taxa. We also note that on FUN4 and FUN5, *Funisia* fossils are represented only by their holdfast 'buds', rather than by the complete Funisia tubular organism (76).A group consisting of all the sessile taxa on the KS surface was also assessed since abundance was not sufficient to include all taxa individually. Taxa were excluded from analyses if there were fewer than five specimens on the surface, because low abundance taxa would fall below the threshold for which results would be statistically meaningful.

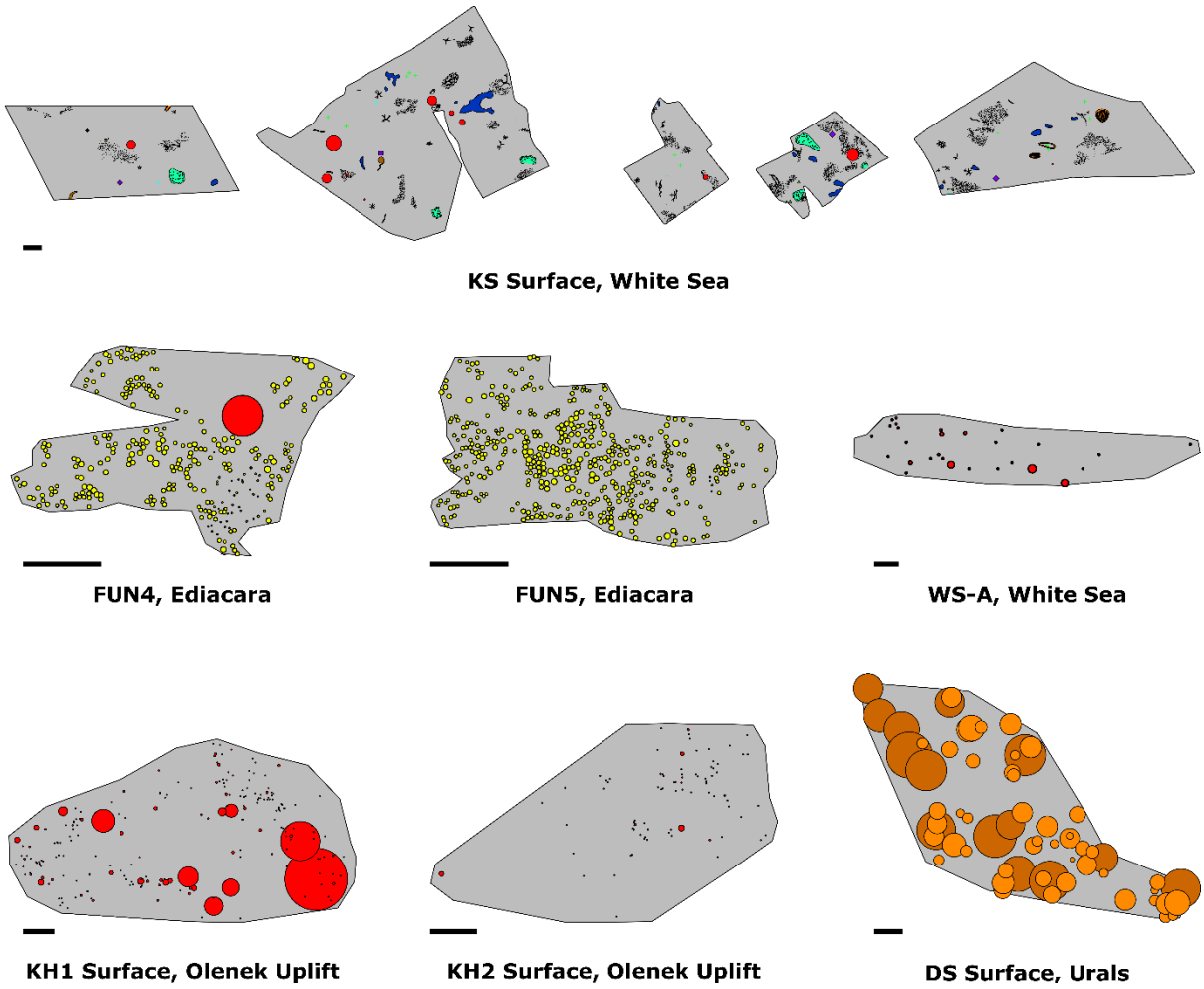

Fig 2. Spatial maps of the seven studied palaeocommunities. Scale bar = 10 cm. Different colours indicate different trace and body fossils as follows: Red, *Aspidella;* Orange, *Dickinsonia;* Yellow circles, *Funisia;* Light green scratch marks, *Kimberichnus;* Light green crosses, *Kimberella;* Blue crosses, *Charniodiscus*; Green triangles, *Parvancorina;* Dark blue patches, *Orbisiana;* Black stipples, horizontal traces; White globular strings, *Palaeopasichnus*; Purple diamonds, *Andiva*; Purple squares, *Yorgia*. Size of the circles corresponds to specimen length or diameter (as appropriate). On the DS surface, dark orange circles are the large size-class of *Dickinsonia*, and the light orange represents the small size-class. See Fig S3 for a high resolution image of the KS surface.

Methods

Bias analyses

For each surface, we first investigated erosional biases by testing to see if fossil density is correlated with sources of modern erosion, such as distance of the surface from the ground, or from a water source (18,72). Since the preserved palaeo-communities are a sub-sample of the communities alive at the time, we would not expect specimen densities to correlate with modern bedding-plane features unless these features were affecting the fossil distributions. Tectonic deformation was tested for by inspection of specimen and bedding-plane deformation (18,72). If these factors were found to have significantly affected specimen density distributions, the erosion and/or deformation were taken into account when performing later analyses cf (. 23), with heavily eroded sections of the bedding planes excluded from analyses. The influence of tectonic deformation was only observed on the DS surface, so retrodeformation techniques (18,25) were not applied to the spatial maps of WS-A, KH1, KH2, KS, FUN4 and FUN5 surfaces. Where possible (WS-A, KH1 and KH2 surfaces), the area near the outcrops was investigated, and no independent evidence of tectonic deformation was found. The holdfast discs on surfaces KS, FUN4 and FUN5 did not show any evidence of tectonic deformation. The DS surface showed signs of deformation in the form of consistent variation in specimen length to width ratios along a presumed axis of deformation. The `fitModel` function from the `mosaic` package in R (73) was used to find the best-fit values for the direction and strength of deformation using the assumption that *Dickinsonia* had a consistent length to width ratio during its ontogeny (40,77,78) though note (79), and the spatial map was retrodeformed (cf. 18,23,25).

Spatial Analyses

Initial data exploration, inhomogeneous Poisson modelling, and segregation tests were

335 performed in R (80) using the package *spatstat* (81,82). Programita software was used to
336 obtain distance measurements and to perform aggregation model fitting (described in detail in
337 references (45,49,81,83–87).
338
339 Univariate and bivariate pair correlation functions (PCFs) were calculated from assemblage
340 population densities using a grid of 1 cm × 1 cm cells on all surfaces except DS, where a 10
341 cm × 10 cm cell size was used to correspond to the larger overall mapped area. To
342 minimise noise, a 3 cell smoothing was calculated dependent on specimen abundance, which
343 was applied to the PCF . To test whether the PCF exhibited complete spatial randomness
344 (CSR), 999 simulations were run for each univariate and bivariate distribution, with the 49
345 highest and 49 lowest values removed . CSR was modelled by a Poisson model on a
346 homogeneous background where the PCF = 1 and the fit of the fossil data to CSR was
347 assessed using Diggle's goodness-of-fit test . Note that due to non-independence of spatial
348 data, Monte-Carlo generated simulation envelopes cannot be interpreted as confidence
349 intervals. If the observed data fell below the Monte-Carlo simulations, the bivariate
350 distribution was interpreted to be segregated; above the Monte-Carlo simulations, the
351 bivariate distribution was interpreted to be aggregated .
352
353 If a taxon was not randomly distributed on a homogeneous background, and was aggregated,
354 the random model on a heterogeneous background was tested by creating a heterogeneous
355 background from the density map of the taxon under consideration. This density map was
356 defined by a circle of radius R over which the density was averaged throughout the sample
357 area. Density maps were formed using estimators within the range of 0.1 m < R < 1 m, with
358 R corresponding to the best-fit model used. If excursions outside the simulation envelopes

for both homogeneous and heterogeneous Poisson models remained, then Thomas cluster models were fitted to the data as follows:

1. The PCF and L-function *(88)* of the observed data were found. Both measures were calculated to ensure that the best-fit model is not optimized towards only one distance measure, and thus encapsulates all spatial characteristics.
2. Best-fit Thomas cluster processes *(89)* were fitted to the two functions where PCF > 1. The best-fit lines were not fitted to fluctuations around the random line of PCF = 1 in order to aid good fit about the actual aggregations, and to limit fitting of the model about random fluctuations. Programita used the minimal contrast method to find the best-fit model.
3. If the model did not describe the observed data well, the lines were re-fitted using just the PCF. If that fit was also poor, then only the L-function was used.
4. Ninety nine simulations of this model were generated to create simulation envelopes, and the fit checked using the O-ring statistic *(83)*.
5. In order to assess how well the model fit the observed data, the goodness-of-fit (p_d) was calculated over the model range *(87)*. A $p_d = 0$ indicates no model fit, and $p_d = 1$ indicates a perfect model fit. Very small-scale segregations (of the order of specimen diameter) were not included in the model fitting, since they likely represent the finite size of the specimens, and a lack of specimen overlap.
6. If there were no excursions outside the simulation envelope and the p_d-value was high, then a univariate homogeneous Thomas cluster model was interpreted as the best model.

For any univariate distributions exhibiting CSR, the size-classes of each taxon were calculated, the univariate PCFs of the smallest size-classes and largest size-classes were plotted, with 999 Monte Carlo simulations of a complete spatially random distribution and

segregation tests performed. The most objective way to resolve the number and range of size classes in a population is by fitting height-frequency distribution data to various models, followed by comparison of (logarithmically scaled) Bayesian information criterion (BIC) values *(87)*, which we performed in R using the package `MCLUST` *(90)*. The number of populations identified was then used to define the most appropriate size classes. A BIC value difference of >10 corresponds to a "decisive" rejection of the hypothesis that two models are the same, whereas values <6 indicate only weakly rejected similarity of the models *(90–94)*. Once defined, the PCFs for each size class were calculated.

Bivariate analyses were performed on the KS surface (the only surface with multiple abundant taxa/taxon groups) between *Kimberella – Orbisiana*, *Kimberella – Kimberichnus* and *Orbisiana – Kimberichnus*. For each 'taxon' pair, the bivariate PCF was calculated, and then compared to CSR using Monte Carlo simulations and Diggle's goodness-of-fit test.

Results

Across the seven palaeocommunities, *Dickinsonia* on the DS surface was the only taxon that exhibited CSR (Table 2). There were five univariate distributions (Sessile Taxa on KS, *Funisia* on FUN4 and FUN5, *Aspidella* on KH1 and KH2) exhibiting aggregated spatial distributions, and two univariate (*Aspidella* on WS-A and large *Dickinsonia* on DS) and one bivariate (*Kimberella* and *Kimberichnus* on KS) segregated spatial distributions (Fig. 3, Table 2). The *Aspidella* aggregations from KH1 and KH2 were best modelled by the same double Thomas cluster process ($p_d^{kh1} = 0.883$, $p_d^{k21} = 0.932$, Fig. 3G, H; Table 2), which consisted of large clusters of 20.96 cm diameter containing smaller clusters with a mean of six specimens within a cluster of 7.34 cm in diameter (Fig. 3G and H, (95)). These results indicate that the non-random spatial distributions were most likely due to two generations of reproduction cf. (44), and do not represent a significant interaction or association with local habitat variations. This

result is consistent with previous work on older (~565 Ma) deep-water communities that also show a strong non-environmentally influenced signal (23). In contrast, the *Aspidella* from the WS-A surface show significant segregation and are best-modelled by a heterogeneous Poisson process ($p_d^{WS\text{-}A} = 0.796$, Fig 3F, Table 2). This is consistent with small-scale intra-specific competition in a resource-limited environment (96). *Funisia* from FUN4 and FUN5 had aggregations that are best-modelled by heterogeneous Poisson processes ($p_d^{Fun4} = 0.9570$, $p_d^{Fun5} = 0.9080$, Fig. 3 D, E; Table 2), which are interpreted to indicate significant habitat associations with the local environment.

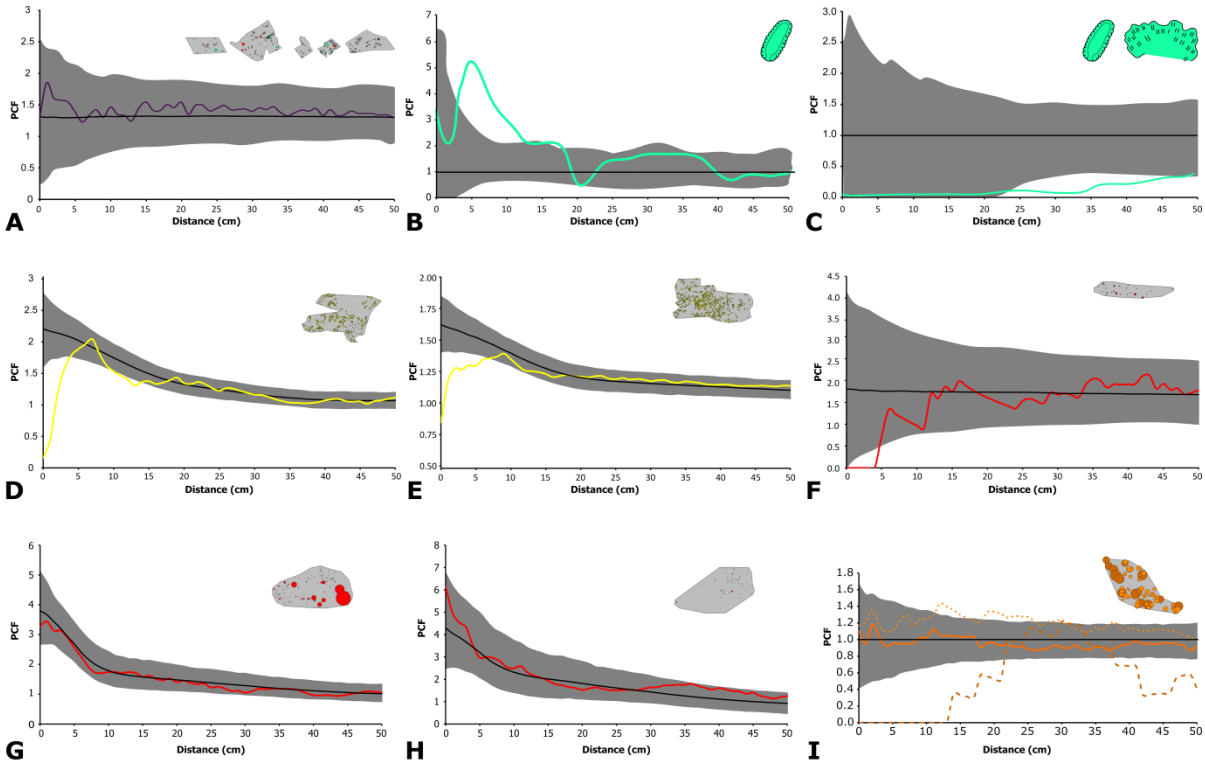

Fig. 3. Pair correlation functions describing the spatial distributions of the seven studied palaeocommunities. The coloured lines are the observed data and black lines represent best-fit models (either CSR or heterogeneous Poisson). The grey area is the simulation envelope for 999 Monte Carlo simulations. The x-axis is the inter-point distance between organisms in centimetres. On the y-axis, PCF = 1 indicates complete spatial randomness (CSR), < 1 indicates segregation, and > 1 indicates aggregation. A) The KS surfaces showing sessile specimens with

the black-line showing the best-fit heterogeneous Poisson model. B) KS univariate *Kimberella*. C) KS bivariate *Kimberella – Kimberichnus* with the CSR model shown. D) FUN4, and E) FUN5 surfaces showing the *Funisia* distributions with the best-fit heterogeneous Poisson model. *Aspidella* from F) WS-A, G) KH1 and H) KH2 surfaces with their best-fit heterogeneous Poisson models. I) *Dickinsonia* from DS with the solid line showing the whole population, dotted line the juveniles and dashed line the adults with the CSR model shown.

SURFACE	TAXON	N	P_d values				
			CSR	HP	TC	DTC	ITC
WS-A	*Aspidella*	40	0.019	**0.796**	0.504	0.2759	0.425
KH1	*Aspidella*	204	0.001	0.001	0.648	**0.883**	0.313
KH2	*Aspidella*	81	0.001	0.001	0.576	**0.932**	0.001
FUN4	*Funisia*	290	0.001	**0.9570**	0.6340	NA	0.245
FUN5	*Funisia*	482	0.001	**0.9080**	0.1320	NA	0.218
DS	*Dickinsonia*	62	**0.857**	0.022	0.025	NA	0.019
	Dickinsonia Small	48	0.128	**0.978**	0.143	NA	0.158
	Dickinsonia Large	14	0.388	0.446	0.409	NA	0.434
KS	All	107	**0.858**	0.381	0.328	NA	0.380
	All sessile	44	0.033	**0.956**	0.770	NA	0.761
	Kimberella	18	0.001	**0.837**	0.491	NA	0.103
	Orbisiana	16	0.325	**0.332**	0.326	NA	0.288
	Kimberichnus	6	**0.566**	NA	NA	NA	NA
	Bivariate *Kimberella – Kimberichnus*	24	**0.028**	NA	NA	NA	NA

Table 2. Goodness-of-fit tests for spatial analyses. For the inhomogeneous point processes (HP and ITC), the moving window radius is 0.5 m, using the same taxon density as the taxon being modelled. $p_d = 1$ corresponds to a perfect fit of the model to the data, while $p_d = 0$ corresponds to no fit. Where observed data did not fall outside CSR Monte-Carlo simulation envelopes, no further analyses were performed, which is indicated by NA. CSR: Complete spatial randomness; HP: Heterogeneous Poisson model; TC: Thomas cluster model; DTC: double Thomas Cluster; ITC: Inhomogeneous Thomas cluster model. N is the number of specimens mapped. Note that for the mobile taxa *Dickinsonia* and *Kimberella*, and presumed trace fossils formed by mobile taxa (*Kimberichnus*), the observed spatial pattern will also be defined by their behaviour, and so the inference of process from pattern is not as

straightforward (see discussion in the main text). The p_d-value of the best-fit model is given in bold.

The KS community is notably different in species composition from deep-water communities because it contains mobile organisms such as *Kimberella* and *Yorgia* (97–100) as well as putative trace fossils such as *Kimberichnus* (thought to be produced by the grazing activity of *Kimberella* specimens) (101). We found that the KS community exhibits CSR, which suggests that any taxon-specific univariate distributions are likely to be biological/ecological in origin, rather than resulting from a taphonomic bias ($p_d{}^{KS}{}_{All} = 0.858$, Table 2, (23)). In contrast, when all the sessile taxa were grouped together they exhibited a significant aggregation (Table 2), which was best-modelled by a heterogeneous Poisson process ($p_d{}^{KS}{}_{Sessile} = 0.956$, Table 2). *Kimberella* exhibits a significant aggregation under spatial scales of 20 cm ($p_d{}^{KS}{}_{Kimberella} = 0.001$ for CSR model, Fig. 3A), with Thomas cluster and heterogeneous Poisson models fitting the data well, suggesting that behavioural factors may also influence *Kimberella* spatial patterns. The *Kimberichnus* PCF spatial distribution has a CSR distribution (Fig. 3B, $p_d{}^{KS}{}_{Rad} = 0.566$, Table 2). Furthermore, the bivariate analyses between *Kimberella* and *Kimberichnus* show a significant segregation ($p_d{}^{KS}{}_{KimRad} = 0.028$, Fig. 3C), which could reflect the *Kimberella* organisms avoiding patches of the surface that had already been grazed.

The *Dickinsonia* population from DS exhibited a CSR PCF distribution (Fig. 3I, $p_d = 0.857$). Previous analysis of the population of *Dickinsonia* from DS showed two cohorts in the size-distribution (95). The two cohorts exhibited different PCF spatial behavior, with the small specimens aggregating with a best-fit heterogeneous Poisson model (Fig. 3I, $p_d^{small} = 0.978$) and the large specimens exhibiting segregation (Fig. 3I).

Interpreting the spatial distributions of mobile organisms

For mobile organisms, inferring the underlying process behind the observed spatial distributions is imprecise, since their spatial patterns also incorporate contributions from their behaviour. Modern animals move primarily to find resources, mates, microhabitats and/or escape predators or detrimental environmental conditions. There is no direct evidence of predators in the Ediacaran, unless perforations in the terminal Ediacaran calcareous tubes of *Cloudina* could be referred to as borings (102). The lack of resolution of reproductive strategies of *Dickinsonia* means that we cannot predict resultant spatial patterns, and thus cannot definitively rule reproductive processes out as a source of spatial patterning. Such reproduction may or may not include necessity for close proximity and/or broadcast spawning cf. the majority of benthic organisms (103). However, reproductive processes are considered unlikely explanation for the observed spatial patterns because the *Dickinsonia* do not aggregate as might be expected in a mating event as demonstrated by the univariate of the largest size-class in the studied *Dickinsonia* population segregation (Fig. 3C, Table 2). Furthermore, broadcast spawning does not require the two mating organisms to be within the spatial scale (< 40 cm) found on the DS surface. We cannot determine whether the large *Dickinsonia* are reacting to the mortality event that killed and preserved them, however, this would not explain the complex interplay between aggregation and segregated behaviors. Therefore, for this *Dickinsonia* population, the search for resources and/or microhabitats is considered the most plausible explanation, particularly since this hypothesis is further supported by their spatial patterns. Aggregated – segregated PCF patterns such as those seen in our *Dickinsonia* population are common in extant sessile organisms where juveniles are initially aggregated on preferred habitats but then begin to compete with each other as they require greater resources, leading to thinning or segregation amongst adult populations. While it is not possible to confirm the underlying mechanism for the distribution of the studied *Dickinsonia* population,

given the preceding points we consider it most likely to be motivated by associations with preferential habitat for food and/or resources. Further analyses of other *Dickinsonia* surfaces would enable more robust conclusions to be reached.

Time averaging

The preservation of time-averaged communities has the potential to bias our analyses (see (21,25). In Avalonian communities, taphomorphs interpreted to record the decaying remains of organisms are identified by their poor preservational fidelity, irregular morphologies, and often high topographic relief (104). This interpretation is consistent with data suggesting that the spatial interactions of some taphomorph populations mirror those of other taxa they are considered to be derived from (21). Taphomorphs are considered unlikely to have imparted a significant signal on these studied surfaces, since we did not observe ivesheadiomorph-type forms, and there is a consistent level of preservational detail amongst fossil communities

Funisia communities tend to have very similar diameters for the holdfasts, which suggests single colonization events (76). Different reproductive events can be distinguished by population analyses of size-distributions (105), with each reproductive event identified through statistically significant cohorts within the size-distribution (90). Surfaces FUN4 and FUN5 both exhibit populations with two cohorts (Fig. S4), most likely indicating two reproductive/colonization events. The best-fit models for each of these surfaces are heterogeneous Poisson models (Fig. 3, Table 2), with very high goodness-of-fit values (p_d > *0.90*) reflecting a single model for each surface. Therefore, cohorts of *Funisia* specimens on each of the studied surfaces were affected by the same underlying environmental heterogeneity, so most likely were contemporaneous.

Discussion

The univariate and bivariate analyses exhibited by taxa within of five out of seven of the studied palaeocommunities provide compelling evidence that their local environment had a significant influence on their communities (Fig. 3, Table 2). In modern settings, habitat associations form when a patchy resource provides heterogeneously distributed preferential conditions for the establishment and growth of sessile taxa, and/or feeding 'hotspots' for mobile taxa . The presence of inferred habitat interactions within our palaeocommunities showed a significant correlation with the environmental setting (Kruskal-Wallis Test, $p = 0.049$), with all five palaeocommunities with strong habitat interactions derived from depositional environments that we consider to be shallow-water settings. The two communities that were seemingly not strongly influenced by their local habitat are from deep-water facies (Table 2). These results are consistent with previous work, which found that for seven independent deep-marine (slope and basin) Ediacaran palaeocommunities from Newfoundland and Charnwood Forest, only one was dominated by associations of taxa with local habitat heterogeneities (21–23) (Kruskal-Wallis Test of all data, $p = 0.021$; Fig. 4).

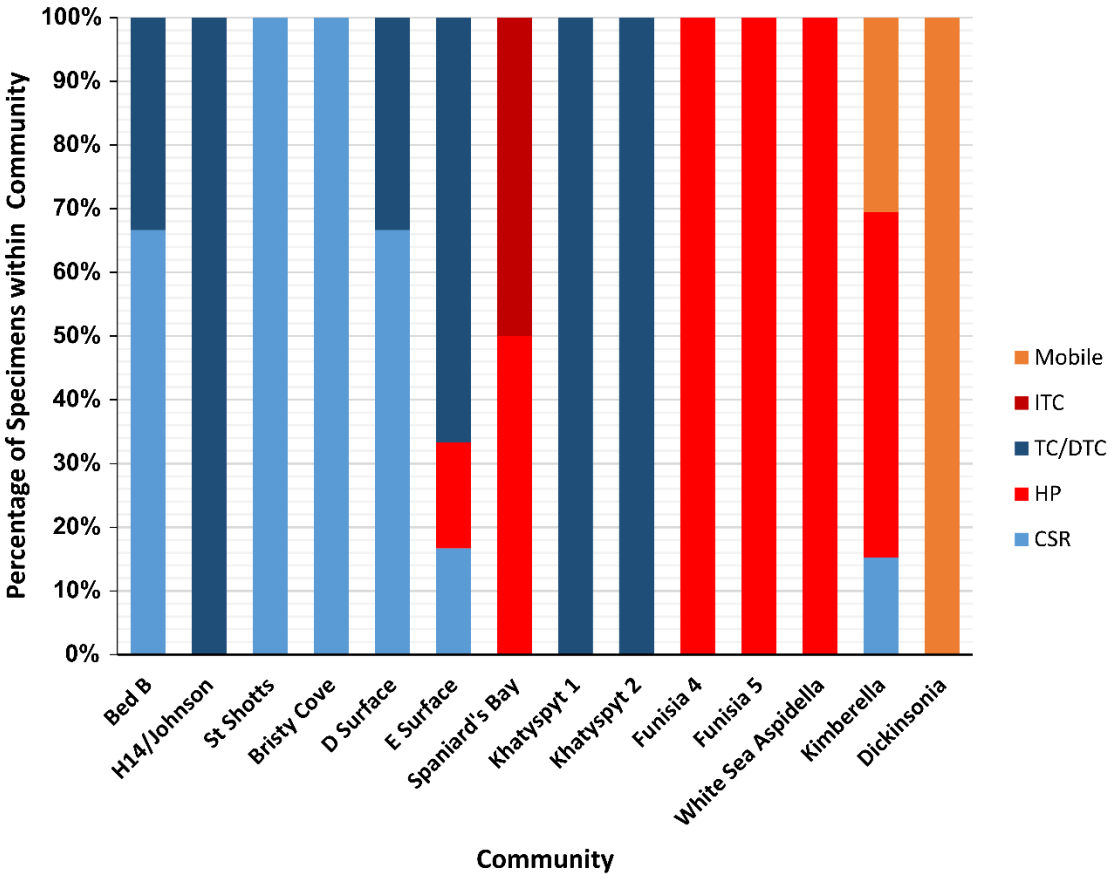

534

535 **Fig. 4 Proportion of best-fit univariate models by surface, adapted from** (23). The
536 percentage of studied body-fossil specimens within the community with univariate spatial
537 distributions that are best described by CSR, HP, TC (or DTC) and ITC models. CSR and TC
538 are considered random or dispersal (neutral) models and are shown in blue. HP and ITC are
539 local environmentally driven (niche) models, shown in red. Mobile taxa are shown in orange,
540 and inferred to be environmentally-driven. Data and plot for surfaces Bed B to Spaniard's Bay
541 from ref. .

542

543 Untangling environmental from evolutionary trends in the Ediacaran has been hampered by a
544 limited overlap between temporal periods and environmental settings (1,17). The
545 palaeocommunities in this study derive from successions containing a variety of lithologies
546 (tuff, coarse sandstone, mixed siltstone, limestone) and reflecting different palaeogeographic

positions (17,57,64,65,76,106,107). We find no significant direct correlations between these factors and the relative importance of habitat heterogeneities on the studied surfaces ($p >> 0.1$; Fig. 3, Table 2). The palaeocommunities that are not influenced by local habitat heterogeneities (KH1 and KH2) are hosted within carbonate successions (107), making them distinct from the siliciclastically-hosted palaeocommunities on the KS, WS-A, FUN4, FUN5 and DS surfaces, or in previous work (21–23). However, the Khatyspyt surfaces behave ecologically in the same way to Avalonian palaeocommunities derived from similar depths, but different lithological successions (21–23), suggesting that lithology alone may not be responsible for the KH1 and KH2 surfaces differing results. Therefore, two possible factors remain that may explain the differences in community dynamics found here. The differences could reflect evolutionary trends, and it is true that the oldest studied palaeocommunities show limited habitat influence (21–23) when compared to the younger palaeocommunities documented in this study (Fig. 4). Unfortunately, the lack of fine-scale dating across these communities and older Avalonian ones precludes detailed fine-scale regression to assess whether the Khatyspyt palaeocommunities are an outlier to this apparent trend, or this trend merely reflects the biases of the available data. Alternatively, the differences could be due to the environmental setting. We have shown that Ediacaran environmental setting has a significant influence on community dynamics ($p = 0.021$), with shallow water palaeocommunities significantly influenced by habitat heterogeneities, in contrast to the deep water palaeocommunities (Fig. 3, Table 2; 21–23). This result does not preclude a simultaneous temporal influence, but given our dataset we are limited to only assessing the broad environmental factor. Our dataset also precludes a more detailed analysis of the relationship between community ecologies with different environmental facies, hence the focus on broad signals (shallow/deep). The surfaces included in this study consist of a small proportion of the known Ediacaran palaeocommunities, and were frequently depauperate in taxonomic diversity,

572 so in order to fully corroborate the proposed hypotheses, analysis of more surfaces from a wider
573 range of global localities is required.
574
575 While SPPA have only been applied to a small proportion of the known *in situ* Ediacaran
576 palaeocommunities (17 studied surfaces to date), there is a notable correspondence between
577 the importance of habitat heterogeneities to community ecology and assemblage diversity. In
578 this study, the palaeocommunities exhibiting significant influence from local habitat
579 heterogeneities belong to the diverse White Sea assemblage, in contrast to the previous work
580 on Avalonian palaeocommunities (21–23), which are not significantly influenced by such
581 heterogeneities. The relationship between environmental spatial heterogeneities and species
582 richness is well established, with habitat variations enabling species to co-exist through the
583 creation of different niches (108). This relationship extends to modern deep-sea benthic
584 communities, where these heterogeneities have been shown to provide a mechanism for
585 diversification on large scales, such as between canyons, trenches and seamounts (109,110),
586 on the centimetre to metre scale (111), and through microhabitats (42).
587
588 In the modern oceans there are three relevant mechanisms that increase habitat heterogeneity,
589 and they do so through increasing both substrate heterogeneity and variation in differentiated
590 particulate organic carbon (POC) and matter (POM) within the water column. First, metazoan
591 mat grazing creates substrate heterogeneity in microbial substrates through the formation of
592 depleted and non-depleted patches (112). Secondly, this grazing induces creation of different-
593 sized detrital particles in the form of differential-sized fecal pellets and fragments of non-
594 consumed food within the water-column, leading to water-column heterogeneity (113).
595 Differential POC and POM create new food sources and therefore new niches, and have been
596 shown to increase the biodiversity of sessile benthic communities (114–116). Thirdly, the main

source of deep-sea habitat heterogeneity is small-scale variation due to differentiated particle influx, with diurnal vertical migration of mesozooplankton and macrofauna contributing up to ~50% of POC to the modern deep-sea via fecal pellets (117–119), with the remaining ~50% transported from shallow to deep-water via oceanic currents (120). Taken together, these modern processes describe how grazing in the shallow waters contributes to habitat heterogeneity in deep-water communities in the form of differentiated POC/POM.

Tentatively, we propose that the ecological differentiation observed between Ediacaran shallow and deep-water communities may evidence the late Ediacaran development of a similar chain of evolutionary diversification. This chain started in shallow water communities, with the creation of habitat patchiness by mobile Ediacaran organisms, which then led to a feedback of increasing diversification that ultimately expanded into the deep-sea. This hypothesized feedback could have promoted diversification through the latest Ediacaran by increasing heterogeneity. First, our data suggest that once grazing had occurred, organisms such as *Kimberella* may have avoided pre-grazed patches (Fig. 3C, Table 2), with this selective grazing accelerating further creation of mat heterogeneity and water-column heterogeneity via differentiated POC (cf. 111,112). Secondly, this differentiated POC and POM would have been transported to the deep-sea via oceanic currents (120). Diurnal vertical migration was likely absent (6) in the Ediacaran, because while a planktonic/larval stage for Ediacaran organisms has been predicted on the basis of their likely waterborne dispersal strategies (25,105), there is presently no direct evidence of non-larval, planktotrophic zooplankton until the onset of the Cambrian . In the absence of planktotrophic zooplankton and widespread pelagic macrofauna, the Ediacaran POC flux may have been either larger, due to lack of consumption of phytoplankton in the shallow water, or smaller, due to a lack of mixing by diurnal vertical migration of the plankton (6), and this cannot yet be determined. Prior to

622 grazers and detritivores, the POC/POM flux would have been dominated by relatively
623 homogenous phytodetritus. The evolution of grazers would have led to a shift towards size-
624 differentiated POC/POM, potentially increasing the heterogeneity of the deep-sea habitat via
625 water-column heterogenization (114–116), and so providing a mechanism for deep-marine
626 diversification.
627
628 Budd and Jensen (12) introduced the Savannah hypothesis to explain early animal
629 diversification, whereby early bilaterian diversification was driven by small-scale variations in
630 local habitat, primarily caused by the spatial distributions of sessile organisms. They argue that
631 it was the drive to find these heterogeneous distributed resources that led to novel evolutionary
632 innovations such as mobility. Our results demonstrate that at least some of the early animal
633 communities that contain mobile organisms were influenced by habitat variations, but the
634 limited number of studied surfaces means that we cannot test whether the observed patchiness
635 results from the spatial distributions of the sessile organisms, or another source. However, we
636 do describe a mechanism that links early animal diversification and benthic habitat patchiness
637 prior to the evolution of predators and wide-spread pelagic organisms. We show that taxa
638 such as *Kimberella* had a segregated distribution with trace fossils considered to be their
639 grazing traces (99), suggesting that they may have been capable of avoiding non-preferred
640 areas (possibly already consumed patches), revealing adaptation of behavior when interacting
641 with these patches. This adaptation theoretically has the capacity to drive further
642 diversification, initially dependent on the environmental-setting, starting in shallow water
643 depositional environments, and then, over time, moving into deeper water, but currently
644 available global fossil assemblages limit the testing of this prediction. If this hypothesis is
645 correct, we would expect deep-water assemblages to diversify during the terminal Ediacaran
646 and into the Cambrian. Our results therefore provide tentative support for the Savannah

647 hypothesis, suggesting that this late Ediacaran taxonomic diversification was a benthic event,
648 which facilitated a chain of diversification by promoting marine habitat heterogeneities.
649

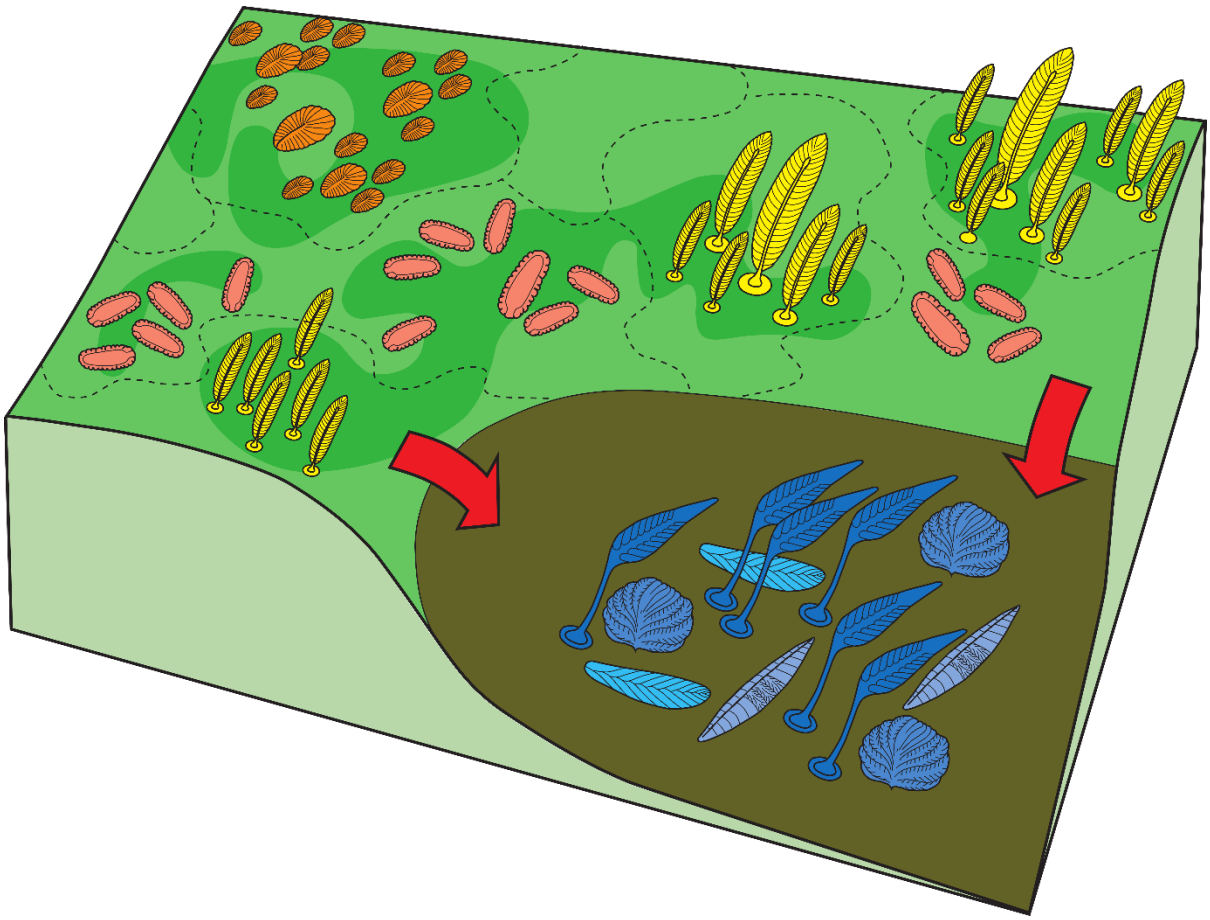

650
651 **Fig. 5. Schematic diagram showing variation of heterogeneities within different**
652 **environmental settings.** Shallow water communities are significantly influenced by habitat
653 heterogeneities. Grazing within these shallow waters further increases substrate heterogeneity,
654 potentially increasing diversification. Furthermore, this grazing increases deep-water
655 heterogeneity through the creation of different sized particulate organic matter due to the influx
656 of particulate matter from the shallows, offering a potential mechanism via which to drive
657 deep-marine diversification.
658
659

Conclusions

We present evidence to suggest that the influence of local habitat on Ediacaran organisms is significantly correlated with broad-scale environmental setting. The relationship of Ediacaran communities to habitat-dependent interactions is correlated with Ediacaran assemblage diversity, with communities from the more diverse White Sea assemblage showing significant habitat associations and interactions in contrast to relatively habitat insensitive deep-sea Avalonian assemblages. We suggest that the presence of shallow-water grazers could have created further habitat heterogeneity in shallow-water and ultimately deep-water, via the heterogenization of the shallow-water substrate and via the introduction of variable size particulate matter to the deep-sea. These results demonstrate the utility of these approaches for investigating the early diversification of metazoans. We have shown the importance of local environmental patchiness to the diversification of early animals, and our results are consistent with the hypothesis that the early diversification of metazoans was a benthic event, driven by responses to habitat patchiness.

Acknowledgements

We thank K. Nagovitsin and O. Zharasbayev (IPGG SB RAS) for help with mapping surfaces KH1 and KH2, and J. Gehling and M. Binnie of the South Australia Museum for assisting with access to Australian material.

Funding

This work has been supported by the Natural Environment Research Council [grant numbers NE/P002412/1 and Independent Research Fellowship NE/S014756/1 to EGM, and Independent Research Fellowship NE/L011409/2 to AGL], a Gibbs Travelling Fellowship (2016-2017) from Newnham College, Cambridge, and a Henslow Research Fellowship from

Cambridge Philosophical Society to EGM (2016–2019). Field research in the White Sea Region, Arctic Siberia and Central Urals has been supported by the Russian Science Foundation [grant number 17-17-01241 to DG]. SX acknowledges funding from the NASA Exobiology and Evolutionary Biology Program [80NSSC18K1086]. Large image processing and interpretation of photomontages of the *Dickinsonia* Surface was supported by the Russian Foundation for Basic Research [grant number 19-05-00828 to AVK].

References

1. Wood R, Liu AG, Bowyer F, Wilby PR, Dunn FS, Kenchington CG, et al. Integrated records of environmental change and evolution challenge the Cambrian Explosion. Nat Ecol Evol. 2019;3(4):528–38.
2. Xiao S, Laflamme M. On the eve of animal radiation: phylogeny, ecology and evolution of the Ediacara biota. Trends in Ecology and Evolution. 2009;24(1):31–40.
3. Erwin DH, Laflamme M, Tweedt SM, Sperling EA, Pisani D, Peterson KJ. The Cambrian Conundrum: Early Divergence and Later Ecological Success in the Early History of Animals. Science. 2011 Nov 25;334(6059):1091–7.
4. Lenton TM, Boyle RA, Poulton SW, Shields-Zhou GA, Butterfield NJ. Co-evolution of eukaryotes and ocean oxygenation in the Neoproterozoic era. Nature Geoscience. 2014;7(4):257–65.
5. Butterfield NJ. Macroevolutionary turnover through the Ediacaran transition: ecological and biogeochemical implications. Geological Society, London, Special Publications. 2009;326(1):55–66.
6. Butterfield NJ. Oxygen, animals and aquatic bioturbation: An updated account. Geobiology. 2018;16(1):3–16.

7. Sperling EA, Frieder CA, Raman AV, Girguis PR, Levin LA, Knoll AH. Oxygen, ecology, and the Cambrian radiation of animals. PNAS. 2013 Aug 13;110(33):13446–51.
8. Lenton TM, Daines SJ. The effects of marine eukaryote evolution on phosphorus, carbon and oxygen cycling across the Proterozoic–Phanerozoic transition. Emerging Topics in Life Sciences. 2018;2(2):267–78.
9. Wood R, Erwin DH. Innovation not recovery: dynamic redox promotes metazoan radiations. Biological Reviews. 2018;93(2):863–73.
10. Butterfield NJ. Animals and the invention of the Phanerozoic Earth system. Trends in Ecology & Evolution. 2011 Feb 1;26(2):81–7.
11. Mángano MG, Buatois LA. Decoupling of body-plan diversification and ecological structuring during the Ediacaran–Cambrian transition: evolutionary and geobiological feedbacks. Proceedings of the Royal Society B: Biological Sciences. 2014 Apr 7;281(1780):20140038.
12. Budd GE, Jensen S. The origin of the animals and a 'Savannah' hypothesis for early bilaterian evolution. Biological Reviews. 2017;92(1):446–73.
13. Muscente AD, Boag TH, Bykova N, Schiffbauer JD. Environmental disturbance, resource availability, and biologic turnover at the dawn of animal life. Earth-Science Reviews. 2018 Feb 1;177:248–64.
14. McPeek MA. The Ecological Dynamics of Natural Selection: Traits and the Coevolution of Community Structure. The American Naturalist. 2017 May 1;189(5):E91–117.
15. Waggoner B. The Ediacaran Biotas in Space and Time. Integr Comp Biol. 2003 Feb 1;43(1):104–13.
16. Grazhdankin D. Patterns of distribution in the Ediacaran biotas: facies versus biogeography and evolution. Paleobiology. 2004 Mar 1;30(2):203–21.

17. Boag TH, Darroch SAF, Laflamme M. Ediacaran distributions in space and time: testing assemblage concepts of earliest macroscopic body fossils. Paleobiology. 2016;42(4):574–94.
18. Wood DA, Dalrymple RW, Narbonne GM, Gehling JG, Clapham ME. Paleoenvironmental analysis of the late Neoproterozoic Mistaken Point and Trepassey formations, southeastern Newfoundland. Canadian Journal of Earth Sciences. 2003 Oct 1;40(10):1375–91.
19. Gehling JG, Droser ML. How well do fossil assemblages of the Ediacara Biota tell time? Geology. 2013 Apr 1;41(4):447–50.
20. Clapham ME, Narbonne GM, Gehling JG. Paleoecology of the oldest known animal communities: Ediacaran assemblages at Mistaken Point, Newfoundland. Paleobiology. 2003;29(4):527–44.
21. Mitchell EG, Butterfield NJ. Spatial analyses of Ediacaran communities at Mistaken Point. Paleobiology. 2018 Feb 1;44(1):40–57.
22. Mitchell EG, Kenchington CG. The utility of height for the Ediacaran organisms of Mistaken Point. Nat Ecol Evol. 2018 Aug;2(8):1218–22.
23. Mitchell EG, Harris S, Kenchington CG, Vixseboxse P, Roberts L, Clark C, et al. The importance of neutral over niche processes in structuring Ediacaran early animal communities. Ecology Letters. 2019;22(12):2028–38.
24. Coutts FJ, Gehling JG, García-Bellido DC. How diverse were early animal communities? An example from Ediacara Conservation Park, Flinders Ranges, South Australia. Alcheringa: An Australasian Journal of Palaeontology. 2016 Oct 24;40(4):407–21.
25. Mitchell EG, Kenchington CG, Liu AG, Matthews JJ, Butterfield NJ. Reconstructing the reproductive mode of an Ediacaran macro-organism. Nature. 2015 Aug;524(7565):343–6.
26. Wilby PR, Carney JN, Howe MPA. A rich Ediacaran assemblage from eastern Avalonia: Evidence of early widespread diversity in the deep ocean. Geology. 2011;39(7):655–8.

27. Narbonne GM. The Ediacara Biota: Neoproterozoic Origin of Animals and Their Ecosystems. Annual Review of Earth and Planetary Sciences. 2005;33(1):421–42.
28. Pu JP, Bowring SA, Ramezani J, Myrow P, Raub TD, Landing E, et al. Dodging snowballs: Geochronology of the Gaskiers glaciation and the first appearance of the Ediacaran biota. Geology. 2016;44(11):955–8.
29. Noble SR, Condon DJ, Carney JN, Wilby PR, Pharaoh TC, Ford TD. U-Pb geochronology and global context of the Charnian Supergroup, UK: Constraints on the age of key Ediacaran fossil assemblages. GSA Bulletin. 2015 Jan 1;127(1–2):250–65.
30. Bush AM, Bambach RK, Erwin DH. Ecospace Utilization During the Ediacaran Radiation and the Cambrian Eco-explosion. Quantifying the Evolution of Early Life. 2011;111–33.
31. Shen B, Dong L, Xiao S, Kowalewski M. The Avalon Explosion: Evolution of Ediacara Morphospace. Science. 2008 Jan 4;319(5859):81–4.
32. Liu AG, Mcllroy D, Brasier MD. First evidence for locomotion in the Ediacara biota from the 565 Ma Mistaken Point Formation, Newfoundland. Geology. 2010 Feb 1;38(2):123–6.
33. Gage JD, Tyler PA. Re-appraisal of age composition, growth and survivorship of the deep-sea brittle star *Ophiura ljungman*i from size structure in a sample time series from the Rockall Trough. Mar Biol. 1981 Sep 1;64(2):163–72.
34. Tecchio S, Ramírez-Llodra E, Sardà F, Company JB. Biodiversity of deep-sea demersal megafauna in western and central Mediterranean basins. Scientia Marina. 2011;75(2):341–50.
35. Seilacher A, Grazhdankin D, Legouta A. Ediacaran biota: The dawn of animal life in the shadow of giant protists. Paleontological Research. 2003;7(1):43–54.
36. Droser ML, Gehling JG. The advent of animals: The view from the Ediacaran. PNAS. 2015 Apr 21;112(16):4865–70.

781 37. Duda J-P, Blumenberg M, Thiel V, Simon K, Zhu M, Reitner J. Geobiology of a
782 palaeoecosystem with Ediacara-type fossils: The Shibantan Member (Dengying
783 Formation, South China). Precambrian Research. 2014 Dec 1;255:48–62.
784 38. Chen Z, Chen X, Zhou C, Yuan X, Xiao S. Late Ediacaran trackways produced by
785 bilaterian animals with paired appendages. Science Advances. 2018 Jun 1;4(6):eaao6691.
786 39. Droser ML, Gehling JG, Tarhan LG, Evans SD, Hall CMS, Hughes IV, et al. Piecing
787 together the puzzle of the Ediacara Biota: Excavation and reconstruction at the Ediacara
788 National Heritage site Nilpena (South Australia). Palaeogeography, Palaeoclimatology,
789 Palaeoecology. 2019 1;513:132–45.
790 40. Reid LM, García-Bellido DC, Gehling JG. An Ediacaran opportunist? Characteristics of a
791 juvenile Dickinsonia costata population from Crisp Gorge, South AustraliaJournal of
792 Paleontology. Journal of Paleontology. 2018;92(3):313–22.
793 41. Finnegan S, Gehling JG, Droser ML. Unusually variable paleocommunity composition in
794 the oldest metazoan fossil assemblages. Paleobiology. 2019 May;45(2):235–45.
795 42. Kukert H, Smith CR. Disturbance, colonization and succession in a deep-sea sediment
796 community: artificial-mound experiments. Deep Sea Research Part A Oceanographic
797 Research Papers. 1992 Jul 1;39(7):1349–71.
798 43. Liu AG, Kenchington CG, Mitchell EG. Remarkable insights into the paleoecology of the
799 Avalonian Ediacaran macrobiota. Gondwana Research. 2015 Jun 1;27(4):1355–80.
800 44. Illian DJ, Penttinen PA, Stoyan DH, Stoyan DD. Statistical Analysis and Modelling of
801 Spatial Point Patterns. John Wiley & Sons; 2008. 557 p.
802 45. Wiegand T, Gunatilleke S, Gunatilleke N, Okuda T. Analyzing the Spatial Structure of a
803 Sri Lankan Tree Species with Multiple Scales of Clustering. Ecology. 2007;88(12):3088–
804 102.

805 46. Seidler TG, Plotkin JB. Seed Dispersal and Spatial Pattern in Tropical Trees. PLOS
806 Biology. 2006 Oct 17;4(11):e344.
807 47. Getzin S, Dean C, He F, Trofymow JA, Wiegand K, Wiegand T. Spatial patterns and
808 competition of tree species in a Douglas-fir chronosequence on Vancouver Island.
809 Ecography. 2006;29(5):671–82.
810 48. Lingua E, Cherubini P, Motta R, Nola P. Spatial structure along an altitudinal gradient in
811 the Italian central Alps suggests competition and facilitation among coniferous species.
812 Journal of Vegetation Science. 2008;19(3):425–36.
813 49. Getzin S, Dean C, He F, Trofymow JA, Wiegand K, Wiegand T. Heterogeneity influences
814 spatial patterns and demographics in forest stands. Journal of Ecology. 2008;96(4):807–
815 20.
816 50. Wiegand T, Moloney KA, Moloney KA. Handbook of Spatial Point-Pattern Analysis in
817 Ecology. 1st ed. Chapman and Hall/CRC; 2013.
818 51. Mitchell EG, Kenchington CG, Harris S, Wilby PR. Revealing rangeomorph species
819 characters using spatial analyses. Canadian Journal of Earth Sciences. 2018 Nov
820 1;55(11):1262–70.
821 52. Lin Y-C, Chang L-W, Yang K-C, Wang H-H, Sun I-F. Point patterns of tree distribution
822 determined by habitat heterogeneity and dispersal limitation. Oecologia. 2011 Jan
823 1;165(1):175–84.
824 53. Diggle P, Zheng P, Durr P. Nonparametric estimation of spatial segregation in a
825 multivariate point process: bovine tuberculosis in Cornwall, UK. Journal of the Royal
826 Statistical Society: Series C (Applied Statistics). 2005;54(3):645–58.
827 54. Law R, Illian J, Burslem DFRP, Gratzer G, Gunatilleke CVS, Gunatilleke I a. UN.
828 Ecological information from spatial patterns of plants: insights from point process theory.
829 Journal of Ecology. 2009;97(4):616–28.

55. Comita L, Condit R, Hubbell SP. Developmental changes in habitat associations of tropical trees. Journal of Ecology. 2007;95:482–92.
56. Grazhdankin D. The Ediacaran genus Inaria: a taphonomicl morphodynamic analysis. Neues Jahrbuch für Geologie und Paläontologie - Abhandlungen. 2000 Apr 18;1–34.
57. Grazhdankin DV. Structure and Depositional Environment of the Vendian Complex in the Southeastern White Sea Area. Stratigraphy and Geological Correlation. 2003;11(4):313–31.
58. Schmitz M, editor. In: The Geologic Time Scale 2012. Elsevier; 2012. p. 1045–1082.
59. Martin MW, Grazhdankin DV, Bowring SA, Evans D a. D, Fedonkin MA, Kirschvink JL. Age of Neoproterozoic Bilatarian Body and Trace Fossils, White Sea, Russia: Implications for Metazoan Evolution. Science. 2000;288(5467):841–5.
60. Tarhan LG, Droser ML, Gehling JG, Dzaugis MP. Microbial mat sandwiches and other anactualistic sedimentary features of the ediacara member (Rawnsley quartzite, South Australia): implications for interpretation of the ediacaran sedimentary recordediacaran anactualistic sedimentology. Palaios. 2017 Mar 1;32(3):181–94.
61. Droser ML, Gehling JG, Dzaugis ME, Kennedy MJ, Rice D, Allen MF. A New Ediacaran Fossil with a Novel Sediment Displaced Life Habit. Journal of Paleontology. 2014 ;88(1):145–51.
62. Tarhan LG, Droser ML, Gehling JG, Dzaugis MP. Taphonomy and morphology of the Ediacara form genus *Aspidella*. Precambrian Research. 2015 Feb 1;257:124–36.
63. Reid LM, Payne JL, García-Bellido DC, Jago JB. The Ediacara Member, South Australia: lithofacies and palaeoenvironments of the Ediacara biota. Gondwana Research 2020 80, pp.321-334
64. Grazhdankin DV, Maslov Av, Krupenin Mt, Mustill Tmr. The Ediacaran White Sea biota in the Central Urals. Doklady Earth Sciences. 2005;401A(3):382–5.

65. Grazhdankin DV, Maslov AV, Krupenin MT. Structure and depositional history of the Vendian Sylvitsa Group in the western flank of the Central Urals. Stratigr Geol Correl. 2009 Oct 9;17(5):476.
66. Bobkov NI, Kolesnikov AV, Maslov AV, Grazhdankin D. The occurrence of *Dickinsonia* in non-marine facies. Estudios geológicos. 75(2):e096.
67. Bobrovskiy I, Hope JM, Ivantsov A, Nettersheim BJ, Hallmann C, Brocks JJ. Ancient steroids establish the Ediacaran fossil *Dickinsonia* as one of the earliest animals. Science. 2018 Sep 21;361(6408):1246–9.
68. Fedonkin MA, Simonetta A, Ivantsov AY. New data on *Kimberella*, the Vendian mollusc-like organism (White Sea region, Russia): palaeoecological and evolutionary implications. Geological Society, London, Special Publications. 2007 Jan 1;286(1):157–79.
69. Kolesnikov AV, Liu AG, Danelian T, Grazhdankin DV. A reassessment of the problematic Ediacaran genus *Orbisiana Sokolov* 1976. Precambrian Research. 2018 Oct 1;316:197–205.
70. Knoll AH, Grotzinger JP, Kaufman AJ, Kolosov P. Integrated approaches to terminal Proterozoic stratigraphy: an example from the Olenek Uplift, northeastern Siberia. Precambrian Research. 1995 May 1;73(1):251–70.
71. Pelechaty SM, Grotzinger JP, Kashirtsev VA, Zhernovsky VP. Chemostratigraphic and Sequence Stratigraphic Constraints on Vendian-Cambrian Basin Dynamics, Northeast Siberian Craton. The Journal of Geology. 1996 Sep 1;104(5):543–63.
72. Nagovitsin KE, Rogov VI, Marusin VV, Karlova GA, Kolesnikov AV, Bykova NV, et al. Revised Neoproterozoic and Terreneuvian stratigraphy of the Lena-Anabar Basin and north-western slope of the Olenek Uplift, Siberian Platform. Precambrian Research. 2015 Nov 1;270:226–45.

879 73. Cui H, Grazhdankin DV, Xiao S, Peek S, Rogov VI, Bykova NV, et al. Redox-dependent
880 distribution of early macro-organisms: Evidence from the terminal Ediacaran Khatyspyt
881 Formation in Arctic Siberia. Palaeogeography, Palaeoclimatology, Palaeoecology. 2016
882 Nov 1;461:122–39.
883 74. Vishnevskaya IA, Letnikova EF, Vetrova NI, Kochnev BB, Dril SI. Chemostratigraphy
884 and detrital zircon geochronology of the Neoproterozoic Khorbusuonka Group, Olenek
885 Uplift, Northeastern Siberian platform. Gondwana Research. 2017 Nov 1;51:255–71.
886 75. Cui H, Xiao S, Cai Y, Peek S, Plummer RE, Kaufman AJ. Sedimentology and
887 chemostratigraphy of the terminal Ediacaran Dengying Formation at the Gaojiashan
888 section, South China. Geological Magazine. 2019 Nov;156(11):1924–48.
889 76. Droser ML, Gehling JG. Synchronous Aggregate Growth in an Abundant New Ediacaran
890 Tubular Organism. Science. 2008 Mar 21;319(5870):1660–2.
891 77. Evans SD, Gehling JG, Droser ML. Slime travelers: Early evidence of animal mobility and
892 feeding in an organic mat world. Geobiology. 2019;17(5):490–509.
893 78. Evans SD, Droser ML, Gehling JG. Highly regulated growth and development of the
894 Ediacara macrofossil Dickinsonia costata. Plos One. 2017;
895 79. Evans SD, Huang W, Gehling JG, Kisailus D, Droser ML. Stretched, mangled, and torn:
896 Responses of the Ediacaran fossil Dickinsonia to variable forces. Geology. 2019 Nov
897 1;47(11):1049–53.
898 80. R Core Team. R: A Language and Environment for Statistical Computing. 2017.
899 81. Baddeley A, Rubak E, Turner R, Rubak E, Turner R. Spatial Point Patterns : Methodology
900 and Applications with R. Chapman and Hall/CRC; 2015.
901 82. Berman M. Testing for Spatial Association between a Point Process and Another
902 Stochastic Process. Journal of the Royal Statistical Society: Series C (Applied Statistics).
903 1986;35(1):54–62.

83. Wiegand T, Moloney KA. Rings, circles, and null-models for point pattern analysis in ecology. Oikos. 2004;104(2):209–29.
84. Wiegand T, Wiegand K, Getzin S. Analyzing the Spatial Structure of a Sri Lankan Tree Species with Multiple Scales of Clustering. Ecology. 2007;88(12):3088–102.
85. Wiegand T, Kissling WD, Cipriotti PA, Aguiar MR. Extending point pattern analysis for objects of finite size and irregular shape. Journal of Ecology. 2006;94(4):825–37.
86. Wiegand T, Moloney KA, Naves J, Knauer F. Finding the Missing Link between Landscape Structure and Population Dynamics: A Spatially Explicit Perspective. The American Naturalist. 1999 Dec 1;154(6):605–27.
87. Loosmore NB, Ford ED. Statistical Inference Using the G or K Point Pattern Spatial Statistics. Ecology. 2006;87(8):1925–31.
88. Levin SA. The Problem of Pattern and Scale in Ecology: The Robert H. MacArthur Award Lecture. Ecology. 1992;73(6):1943–67.
89. Besag J. Spatial Interaction and the Statistical Analysis of Lattice Systems. Journal of the Royal Statistical Society: Series B (Methodological). 1974;36(2):192–225.
90. Fraley C, Raftery AE. MCLUST Version 3 for R: Normal Mixture Modeling and Model-Based Clustering∗. 2017;57.
91. Grabarnik P, Myllymäki M, Stoyan D. Correct testing of mark independence for marked point patterns. Ecological Modelling. 2011 Dec 10;222(23):3888–94.
92. Fraley C, Raftery AE. Bayesian Regularization for Normal Mixture Estimation and Model-Based Clustering. Journal of Classification. 2007;24(2):155–81.
93. Pélissier R, Goreaud F. A practical approach to the study of spatial structure in simple cases of heterogeneous vegetation. Journal of Vegetation Science. 2001;12(1):99–108.
94. Chiu SN, Stoyan D, Kendall JM. Stochastic Geometry and Its Applications. 2013.

95. Soznov NG, Bobkov NI, Mitchell EG, Kolesnikov A V, Grazhdankin DV. The ecology of *Dickinsonia* on tidal flats. IMECT 2019. 2019;
96. Kenkel NC. Pattern of Self-Thinning in Jack Pine: Testing the Random Mortality Hypothesis. Ecology. 1988;69(4):1017–24.
97. Ivantsov AYu. Trace fossils of precambrian metazoans "Vendobionta" and "Mollusks". Stratigr Geol Correl. 2013 May 1;21(3):252–64.
98. Ivantsov AYu. Feeding traces of proarticulata—the Vendian metazoa. Paleontol J. 2011 May 1;45(3):237–48.
99. Ivantsov AYu. New reconstruction of *Kimberella*, problematic Vendian metazoan. Paleontol J. 2009 Dec 14;43(6):601.
100. Ivantsov A.yu., Malakhovskaya Ya.e. Giant traces of vendian animals. Doklady Earth Sciences. 2002;385(6):618–22.
101. Managano MG, Buatois LA. The Cambrian revolutions: Trace-fossil record, timing, links and geobiological impact. Earth-Science Reviews. 2017 Oct 1;173:96–108.
102. Hua H, Pratt BR, Zhang L-Y. Borings in *Cloudina* Shells: Complex Predator-Prey Dynamics in the Terminal Neoproterozoic. PALAIOS. 2003;18(4–5):454–9.
103. Giangrande A, Geraci S, Belmonte G. Life-cycle and life-history diversity in marine invertebrates and the implications in community dynamics. Oceanographic Literature Review. 1995;8(42):662.
104. Liu AG, Mcilroy D, Antcliffe JB, Brasier MD. Effaced preservation in the Ediacara biota and its implications for the early macrofossil record. Palaeontology. 2011;54(3):607–30.
105. Darroch SAF, Laflamme M, Clapham ME. Population structure of the oldest known macroscopic communities from Mistaken Point, Newfoundland. Paleobiology. 2013;39(4):591–608.

106. Muscente AD, Bykova N, Boag TH, Buatois LA, Mángano MG, Eleish A, et al. Ediacaran biozones identified with network analysis provide evidence for pulsed extinctions of early complex life. Nat Commun 10(1), pp.1-15

107. Grazhdankin DV, Balthasar U, Nagovitsin KE, Kochnev BB. Carbonate-hosted Avalon-type fossils in arctic Siberia. Geology. 2008;36(10):803–6.

108. Ben- Hur E, Kadmon R. Heterogeneity–diversity relationships in sessile organisms: a unified framework. Ecology Letters 23(1), pp.193-207

109. Levin LA, Sibuet M, Gooday AJ, Smith CR, Vanreusel A. The roles of habitat heterogeneity in generating and maintaining biodiversity on continental margins: an introduction. Marine Ecology. 2010;31(1):1–5.

110. Vanreusel A, Fonseca G, Danovaro R, Silva MCD, Esteves AM, Ferrero T, et al. The contribution of deep-sea macrohabitat heterogeneity to global nematode diversity. Marine Ecology. 2010;31(1):6–20.

111. McClain C, Barry JP. Habitat heterogeneity, disturbance, and productivity work in concert to regulate biodiversity in deep submarine canyons. Ecology. 2010;91(4):964–76.

112. Sommer U. Benthic microalgal diversity enhanced by spatial heterogeneity of grazing | SpringerLink. Oecologia. 2000;122:284–7.

113. Stramski D, Rassoulzadegan F, Kiefer DA. Changes in the optical properties of a particle suspension caused by protist grazing. J Plankton Res. 1992 Jan 1;14(7):961–77.

114. Leduc D, Rowden AA, Probert PK, Pilditch CA, Nodder SD, Vanreusel A, et al. Further evidence for the effect of particle-size diversity on deep-sea benthic biodiversity. Deep Sea Research Part I: Oceanographic Research Papers. 2012 May 1;63:164–9.

115. Gili J-M, Coma R. Benthic suspension feeders: their paramount role in littoral marine food webs. Trends in Ecology & Evolution. 1998 Aug 1;13(8):316–21.

977 116. Smith CR, De Leo FC, Bernardino AF, Sweetman AK, Arbizu PM. Abyssal food
978 limitation, ecosystem structure and climate change. Trends in Ecology & Evolution. 2008
979 Sep 1;23(9):518–28.
980 117. Manno C, Stowasser G, Enderlein P, Fielding S, Tarling GA. The contribution of
981 zooplankton faecal pellets to deep carbon transport in the Scotia Sea (Southern Ocean).
982 Biogeosciences. 2015 Mar 25;12:1955–65.
983 118. Davison PC, Checkley DM, Koslow JA, Barlow J. Carbon export mediated by
984 mesopelagic fishes in the northeast Pacific Ocean. Progress in Oceanography. 2013 Sep
985 1;116:14–30.
986 119. Giering SLC, Sanders R, Lampitt RS, Anderson TR, Tamburini C, Boutrif M, et al.
987 Reconciliation of the carbon budget in the ocean's twilight zone. Nature. 2014
988 ;507(7493):480–3.
989 120. Monteiro PMS, Nelson G, van der Plas A, Mabille E, Bailey GW, Klingelhoeffer E.
990 Internal tide—shelf topography interactions as a forcing factor governing the large-scale
991 distribution and burial fluxes of particulate organic matter (POM) in the Benguela
992 upwelling system. Continental Shelf Research. 2005 Sep 1;25(15):1864–76.

993